Saunders, A.D., Larsen, H.C., and Wise, S.W., Jr. (Eds.), 1998
Proceedings of the Ocean Drilling Program, Scientific Results, Vol. 152

29. Sr-, Nd-, AND Pb-ISOTOPIC COMPOSITION OF VOLCANIC ROCKS FROM THE SOUTHEAST GREENLAND MARGIN AT 63°N: TEMPORAL VARIATION IN CRUSTAL CONTAMINATION DURING CONTINENTAL BREAKUP[1]

J.G. Fitton,[2] B.S. Hardarson,[2] R.M. Ellam,[3] and G. Rogers[3]

ABSTRACT

The southeast Greenland seaward-dipping reflector sequence (SDRS) is composed of Paleocene to Eocene volcanic rocks erupted during continental breakup. Volcanic rocks recovered from a transect across the SDRS at 63°N, during Ocean Drilling Program Leg 152, range in composition from picrite to dacite and represent all the magmatic phases in the development of the continental margin. The earliest magmas, represented by the pre-breakup succession at Site 917 (Lower and Middle Series), were strongly contaminated with continental crust, but the degree of contamination declined rapidly during the late stages of breakup (Site 917 Upper Series). Very low concentrations of incompatible elements in the uncontaminated primitive magmas made them extremely sensitive to the isotopic effects of crustal contamination. Basaltic rocks from the most seaward part of the transect (Site 918) were erupted after breakup and show no signs of contamination with continental crust. Two distinct crustal contaminants can be recognized: (1) lower crustal basic granulite with unradiogenic Nd, Sr, and Pb; and (2) upper crustal amphibolite-facies gneiss with unradiogenic Nd but highly radiogenic Sr and high $^{208}Pb/^{204}Pb$. The first contaminant affected only the earliest magmas, represented by the lower volcanic units in the Lower Series at Site 917. Later continental magmas were affected by the second contaminant, suggesting storage of magmas at progressively shallower levels in the crust as lithospheric extension proceeded toward continental breakup. The nature and degree of contamination are strikingly similar to those observed in the Hebridean Tertiary igneous province, which would have been adjacent to southeast Greenland during continental breakup.

INTRODUCTION

Ocean Drilling Program (ODP) Leg 152 sampled a transect across the volcanic rocks forming the seaward-dipping reflector sequence (SDRS) off southeast Greenland. These rocks were erupted between 61 and 52 Ma (Sinton and Duncan, this volume) and span the whole period of continental breakup and the development of the continental margin (Larsen, Saunders, Clift, et al., 1994; Fitton et al., 1995). Chemical analyses of volcanic rocks from the Leg 152 transect have been presented by Fitton et al. (this volume), Fram et al. (this volume) and Larsen, Fitton and Fram (this volume).

The earliest, and most landward, lava flows (Hole 917A, Lower and Middle Series) represent a pre-breakup continental sequence showing an overall variation from olivine basalt to dacite. Evolved compositions dominate the upper parts of this sequence, and the lowest dacite unit is used to define the base of the Middle Series. A thin (67 cm) sandstone layer, which may represent a hiatus in volcanism at Site 917, separates the Middle Series from an overlying suite of picrite and olivine basalt flows (Hole 917A, Upper Series) erupted during the final phase of breakup. The younger parts of the SDRS (Sites 915 and 918) comprise compositionally uniform basalt thought to have been erupted from magma chambers associated with an oceanic spreading axis. Volcanic rocks that were erupted during and after breakup (Hole 917A, Upper Series, and Holes 915A and 918D, respectively) record a progressive increase in degree, and decrease in depth, of mantle melting and melt segregation as the lithosphere thinned and finally gave way to seafloor spreading (Fitton et al., this volume; Fram et al., this volume). A thin basaltic sill intruding lower Eocene sands above the lava sequence at Site 918 is the youngest igneous rock sampled in the transect, and is probably related to a small off-axis volcano.

The Lower and Middle Series volcanic rocks at Site 917 show clear indications of contamination of the magmas with continental crust (Larsen, Saunders, Clift, et al., 1994; Fitton et al., this volume). Variation of incompatible-element ratios with SiO_2 content cannot be explained by differentiation of the magmas by fractional crystallization alone, but requires assimilation of a crustal component containing high concentrations of, for example, Zr, light rare-earth elements (LREE), and Ba. A sample of Archaean gneiss collected from an onshore outcrop close to the Leg 152 transect (GGU 324721; Blichert-Toft et al., 1995) represents the type of crustal material that might have been involved. An increase in SiO_2 content upward through the Lower and Middle Series, correlated with indices of crustal contamination, suggests storage, differentiation, and contamination of the magma in crustal magma reservoirs fed with a dwindling supply of primary magma. The Upper Series picrite and olivine basalt flows at Site 917 show only slight evidence, in their trace-element abundances, for crustal contamination. This series represents a resurgence of magmatism accompanying the final stages of breakup of the margin, with near-primary magma erupted rapidly from mantle depths.

Simple fractional crystallization coupled with assimilation of a single crustal component cannot account for all of the variation seen in the Lower and Middle Series. Lava flows forming the lower half of the Lower Series in Hole 917A (below Unit 73A) have higher Sr/Zr and La/Th, and slightly higher Ba/Zr than do the upper flows (Fitton et al., this volume, fig. 10). The lower units require a contaminant that is chemically distinct from that affecting the Middle Series and the upper units of the Lower Series. This paper reports the results of isotopic studies that help to constrain the nature of the contaminants. We will show that the magmas represented by the lower parts of the succession were contaminated with basic granulite, probably in the lower crust, whereas the contaminant affecting later mag-

[1]Saunders, A.D., Larsen, H.C., and Wise, S.W., Jr. (Eds.), 1998. *Proc. ODP, Sci. Results*,152: College Station, TX (Ocean Drilling Program).

[2]Department of Geology and Geophysics, University of Edinburgh, West Mains Road, Edinburgh EH9 3JW, United Kingdom. godfrey.fitton@glg.ed.ac.uk

[3]Scottish Universities Research and Reactor Centre, East Kilbride, Glasgow G75 0QF, United Kingdom.

mas had isotopic characteristics typical of upper crustal amphibolite-facies gneiss.

ANALYTICAL TECHNIQUES

Sr-, Nd-, and Pb-isotope analyses were conducted at the Scottish Universities Research and Reactor Centre (SURRC), East Kilbride, using aliquots of the same rock powders analyzed by Fitton et al. (this volume). To minimize the effects of alteration on $^{87}Sr/^{86}Sr$, the samples were leached in 6M HCl for 6 hr at 170°C, and then washed repeatedly in distilled water before Sr and Nd separation. Leaching for 6 hr was found to give constant $^{87}Sr/^{86}Sr$, with no further change on leaching for 24 hr. Sr was separated from samples using standard cation exchange techniques. Nd was purified from the bulk rare-earth elements (REE) fraction from the cation exchange columns using two further columns. First, the REE were separated from Ba by loading the sample onto a column containing 0.25 ml of EiChrom SrSpec ion exchange resin and eluting with 3M HNO_3, the Ba being retained on the column. Nd was separated from the other REE on a temperature-controlled anion exchange column as described by Barbero et al. (1995).

Sr samples were analyzed on a VG 54E thermal ionization mass spectrometer. $^{87}Sr/^{86}Sr$ was corrected for mass fractionation using $^{86}Sr/^{88}Sr = 0.1194$. Repeat analysis of NBS987 Sr standard gave $^{87}Sr/^{86}Sr = 0.710219 \pm 26$ (2 s.d., $n = 9$), and all data were normalized to a value of $^{87}Sr/^{86}Sr = 0.710243$ for this standard. Nd samples were analyzed on a VG Sector 54-30 thermal ionization mass spectrometer in multi-dynamic mode. $^{143}Nd/^{144}Nd$ was corrected for mass fractionation using $^{146}Nd/^{144}Nd = 0.7219$. During the course of this study the SURRC internal JM Nd laboratory standard gave $^{143}Nd/^{144}Nd = 0.511501 \pm 12$ (2 s.d.).

Unleached powder samples were used for Pb-isotope analysis. Pb was separated by using standard HBr-HCl anion exchange techniques, and analyzed on a VG 54E thermal ionization mass spectrometer. The data were corrected for mass fractionation of 0.1% amu^{-1} based on replicate analysis of the NBS 981 standard. External reproducibility of the Pb isotopic ratios is 0.2% (2 s.d.), and analytical blanks were <1 ng.

RESULTS

Sr- and Nd-isotope ratios were determined on 32 samples, and most of these were also analyzed for Pb-isotope ratios. Samples are identified by site and unit (defined in Larsen, Saunders, Clift, et al., 1994) and these informal sample numbers are keyed to full ODP designations in Table 1. The isotopic data are reported in Table 2; chemical analyses of the same samples are given in Fitton et al. (this volume).

Variation of $^{87}Sr/^{86}Sr$ and $^{143}Nd/^{144}Nd$ in volcanic rocks from the Leg 152 transect is shown in Figure 1. The effects of age-correcting data (to 60 Ma) from the three samples with the highest Rb/Sr (917-47, -55, and -72) are also shown in this figure. These corrections were based on whole-rock Rb/Sr and Sm/Nd (from Fitton et al., this volume). The other data have not been age corrected because of uncertainties in Rb/Sr in the acid-leached residues. This ratio is likely to be lower than in the whole-rock samples, and age correction would therefore be insignificant in comparison with the measured isotopic range. The isotopic composition (measured and age corrected) of a sample of Archaean gneiss collected on shore, close to the Leg 152 transect (GGU 324721; Blichert-Toft et al., 1995), is also shown on this diagram. Dickin's (1981) estimates of average granulite- and amphibolite-facies Lewisian gneiss, corrected to 60 Ma, are included for comparison. These are believed to represent lower and upper continental crust respectively. Variation of $^{143}Nd/^{144}Nd$ with stratigraphic position in the SDRS is shown in Figure 2.

Table 1. Location of samples used in this study.

Sample	Hole, core, section, interval (cm)	Piece	Depth (mbsf)	Series	Unit
915-3	915A-24R-2, 60–64	2B	198.68	Lava	3
917-10	917A-10R-4, 48–51	2A	78.53	Upper	10
917-14	917A-12R-1, 31–36	4A	92.31	Upper	14
917-17	917A-13R-5, 120–124	11	108.19	Upper	17
917-26	917A-18R-4, 105–109	7B	151.04	Upper	26
917-32B	917A-20R-4, 131–134	11	170.06	Upper	32B
917-33	917A-21R-3, 126–130	5	177.75	Upper	33
917-34B	917A-23R-2, 64–68	15	194.01	Middle	34B
917-47	917A-32R-4, 76–80	10	244.82	Middle	47
917-55	917A-51R-1, 42–45	10	365.42	Middle	55
917-58	917A-54R-4, 70–73	1C	388.95	Lower	58
917-60	917A-55R-5, 66–70	9A	399.98	Lower	60
917-61B	917A-57R-3, 67–71	1A	416.36	Lower	61B
917-62	917A-57R-7, 29–32	1B	421.58	Lower	62
917-63	917A-58R-3, 0–5	1A	424.69	Lower	63
917-68	917A-64R-2, 43–47	1B	472.63	Lower	68
917-70	917A-67R-3, 126–130	6B	503.69	Lower	70
917-71	917A-69R-2, 123–127	4	521.53	Lower	71
917-72	917A-71R-4, 27–31	1C	542.07	Lower	72
917-73A	917A-72R-1, 53–57	3D	547.83	Lower	73A
917-74A	917A-74R-1, 41–48	8A	567.11	Lower	74A
917-78	917A-79R-2, 75–79	1D	607.19	Lower	78
917-81B	917A-81R-4, 54–58	6	629.32	Lower	81B
917-88	917A-96R-1, 110–114	10A	760.50	Lower	88
917-89	917A-97R-2, 11–15	1A	770.36	Lower	89
917-90	917A-99R-2, 60–64	1D	790.37	Lower	90
918-1	918D-94R-1, 80–84	4D	1176.20	Sill	1
918-8B	918D-101R-4, 96–100	12	1226.65	Lava	8B
918-12Bi	918D-107R-2, 92–96	12B	1259.58	Lava	12B
918-12Bii	918D-108R-1, 42–46	2B	1262.62	Lava	12B
918-13B	918D-109R-3, 50–54	5	1270.15	Lava	13B
918-15	918D-111R-3, 77–81	9B	1285.12	Lava	15

Several significant features of the isotopic data can be seen on Figures 1 and 2. First, the post-breakup lavas collected from Hole 918D form a tight cluster with $^{143}Nd/^{144}Nd > 0.5130$, values comparable with those from the most depleted basalts in Iceland (Hémond et al., 1993) and some normal mid-ocean-ridge basalt (N-MORB) samples from the Atlantic (Ito et al., 1987). The small but significant range in $^{87}Sr/^{86}Sr$ in the Site 918 samples may be due to the effects of alteration. Most of the samples from the Upper Series at Site 917, two samples from the Lower Series, and the sill from Site 918 also have high $^{143}Nd/^{144}Nd$ and low $^{87}Sr/^{86}Sr$. Second, the lower units of the Lower Series (below Unit 73A; Fig. 2) plot along a trend to low $^{143}Nd/^{144}Nd$ at nearly constant $^{87}Sr/^{86}Sr$, toward the isotopic composition of average granulite-facies Lewisian gneiss (Fig. 1). And third, some of the Lower Series lavas (LSb on Figs. 1, 2), the three Middle Series samples, one sample from the Upper Series, and the sample from Hole 915A, all plot on a trend to low $^{143}Nd/^{144}Nd$ and high $^{87}Sr/^{86}Sr$, consistent with assimilation of material similar to the gneiss sample 324721 and Dickin's (1981) average amphibolite-facies Lewisian gneiss. The LSb samples are from a group of lava flows toward the top of the Lower Series at Site 917, and are chemically distinct from the other Lower Series flows (LSa) in having high Nb/Zr (Fitton et al., this volume). Three LSa flows from the upper part of the Lower Series (Fig. 2) plot between the two trends on Figure 1.

Lead-isotope variation is shown in Figures 3 and 4. These diagrams include data from Icelandic basalt (see Fig. 3 caption for data sources), Precambrian basement rocks of East Greenland (Leeman et al., 1976) and southeast Greenland (Taylor et al., 1992; Kalsbeek et al., 1993), and Dickin's (1981) estimates of the isotopic composition of average granulite- and amphibolite-facies Lewisian gneiss. Samples from Hole 918D and most samples from the Upper Series in Hole 917A plot close to the Iceland data on both diagrams, as would be expected from the low $^{87}Sr/^{86}Sr$ and high $^{143}Nd/^{144}Nd$ in these samples (Fig. 1). The other samples define a tight linear trend toward very unradiogenic Pb on a $^{207}Pb/^{204}Pb$ vs. $^{206}Pb/^{204}Pb$ diagram (Fig. 3), implying contamination of the magma with Archaean crust. The crustal component, however, must be more unradiogenic in $^{207}Pb/^{204}Pb$ than any of the samples of Archaean crust shown in Figure 3. On a $^{208}Pb/^{204}Pb$ vs. $^{206}Pb/^{204}Pb$ diagram (Fig. 4) the data are more scattered, with the Middle and Upper

Table 2. Isotopic data for volcanic rocks from Leg 152.

Sample	Series	$^{87}Sr/^{86}Sr$	2 *se*	$^{143}Nd/^{144}Nd$	2 *se*	$^{206}Pb/^{204}Pb$	2 *se*	$^{207}Pb/^{204}Pb$	2 *se*	$^{208}Pb/^{204}Pb$	2 *se*
915-3	Lava	0.703669	46	0.512878	12	17.228	20	15.381	22	37.575	51
917-10	Upper	0.702992	40	0.513111	9	17.688	6	15.494	8	37.541	19
917-14	Upper	0.703201	20	0.513035	7	16.832	10	15.268	12	37.381	20
917-17	Upper	0.704055	20	0.512613	6	15.433	9	14.826	12	37.114	27
917-26	Upper	0.702993	23	0.513077	7						
917-32B	Upper	0.702997	29	0.513058	16	17.760	15	15.480	14	37.530	30
917-33	Upper	0.703604	24	0.513085	6	17.941	5	15.396	5	37.494	11
917-34B	Middle	0.713970	31	0.511881	6	16.276	10	14.976	18	38.335	36
917-47	Middle	0.710495	28	0.510887	7	13.684	8	14.470	7	35.673	20
917-55	Middle	0.706540	27	0.511268	7	13.757	6	14.467	8	34.749	21
917-58	Lower	0.703876	12	0.512121	9						
917-60	Lower*	0.703299	24	0.512975	8						
917-61B	Lower*	0.703909	39	0.512886	12	17.625	12	15.416	15	37.675	27
917-62	Lower*	0.703922	29	0.512841	7						
917-63	Lower	0.703652	40	0.512240	8	14.781	11	14.715	11	35.126	21
917-68	Lower*	0.704280	23	0.512731	8						
917-70	Lower*	0.704242	32	0.512304	8						
917-71	Lower	0.703559	31	0.512001	9						
917-72	Lower*	0.704579	23	0.512650	6	17.773	5	15.243	4	37.926	13
917-73A	Lower	0.703111	33	0.513113	8	17.625	9	15.446	9	37.541	22
917-74A	Lower	0.703180	38	0.511434	6	13.768	3	14.439	12	33.649	28
917-78	Lower	0.703375	38	0.511559	5						
917-81B	Lower	0.702701	22	0.511859	15	14.132	5	14.558	7	33.960	18
917-88	Lower	0.702968	31	0.511493	9	16.045	3	15.049	4	36.809	10
917-89	Lower	0.702773	27	0.512018	6						
917-90	Lower	0.702822	30	0.511886	7	14.402	3	14.646	4	34.165	11
918-1	Sill	0.702997	28	0.512941	6	18.140	7	15.440	8	38.056	17
918-8B	Lava	0.703734	29	0.513065	6						
918-12B.1	Lava	0.703023	31	0.513134	8	17.789	23	15.582	27	37.650	77
918-12B.2	Lava	0.703048	23	0.513129	7						
918-13B	Lava	0.703003	20	0.513076	7						
918-15	Lava	0.702966	34	0.513054	8	17.889	7	15.486	7	37.864	16

Note: * = samples from the high-Nb/Zr group (LSb) of the Lower Series. The other Lower Series samples belong to the low-Nb/Zr group (LSa).

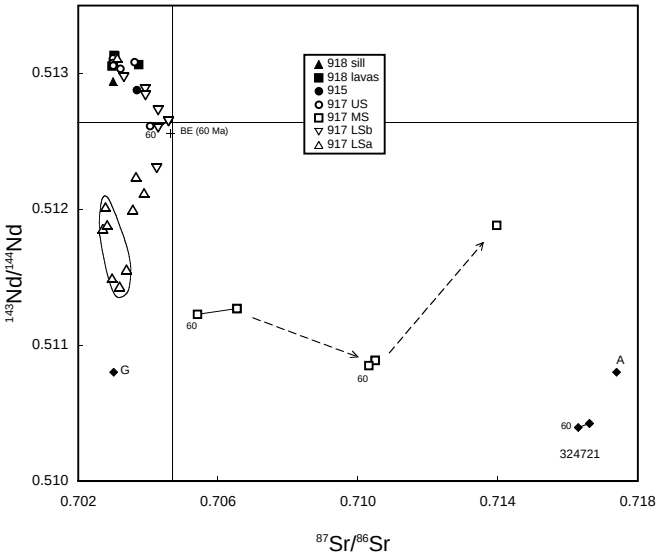

Figure 1. Variation of $^{143}Nd/^{144}Nd$ and $^{87}Sr/^{86}Sr$ in volcanic rock samples recovered during Leg 152. Data for the three most evolved samples (Rb/Sr> 0.07) have been age corrected to 60 Ma (corrected and uncorrected data points joined by tie lines), but data for the other samples are uncorrected. The bulk-earth isotopic composition at 60 Ma (+) is shown for reference. Samples from Site 917 are divided into Lower (LS), Middle (MS), and Upper Series (US), and the Lower Series is subdivided into low-Nb/Zr (LSa) and high-Nb/Zr (LSb) flows (Fitton et al., this volume). The elliptical field encloses data points representing samples from the lower part of the Lower Series at Site 917 (below Unit 73A), the oldest volcanic rocks recovered from the transect. Arrows show the change in isotopic composition upward through the Middle Series succession. Points labelled 324721 represent age-corrected and uncorrected data from a sample of gneiss collected onshore, close to the Leg 152 transect (Blichert-Toft et al., 1995). Average compositions, corrected to 60 Ma, of granulite- (G) and amphibolite-facies (A) Lewisian gneiss (from Dickin, 1981) are shown for comparison.

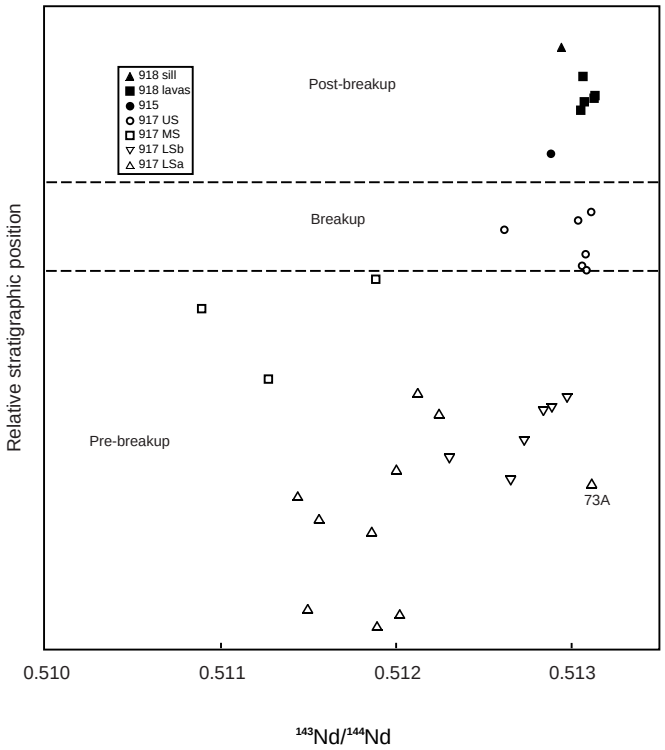

Figure 2. Stratigraphic variation of $^{143}Nd/^{144}Nd$ in volcanic rock samples recovered from the Leg 152 transect (sample identification as in Fig. 1). Data from the three sites are stacked to form a temporal and geographic sequence from the oldest and most landward at the bottom, to the youngest and most seaward at the top. The volcanic sequences plotted for Sites 917 and 918 represent 770 m and 126 m of vertical section, respectively.

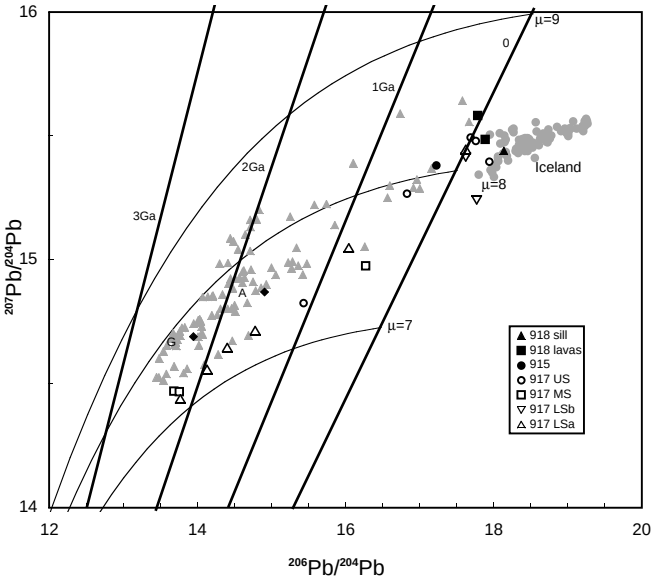

Figure 3. $^{207}Pb/^{204}Pb$ vs. $^{206}Pb/^{204}Pb$ in volcanic rock samples recovered from the Leg 152 transect (sample identification as in Fig. 1). The data have not been age corrected. The isotopic composition of Pb in volcanic rocks from Iceland (gray circles; data from Cohen and O'Nions, 1982; Elliott et al., 1991; Furman et al., 1991; Hards et al., 1995; Park, 1990; Sun and Jahn, 1975; Sun et al., 1975; B.S. Hardarson and R.M. Ellam, unpubl. data), and in Archaean basement rocks (gray triangles) from East Greenland (Leeman et al., 1976) and southeast Greenland (Kalsbeek et al., 1993; Taylor et al., 1992) are shown for comparison. The average compositions of granulite- (G) and amphibolite-facies (A) Lewisian gneiss (from Dickin, 1981) are also shown. Single-stage Pb growth curves ($\mu = {}^{238}U/^{204}Pb$) and isochrons are plotted for reference.

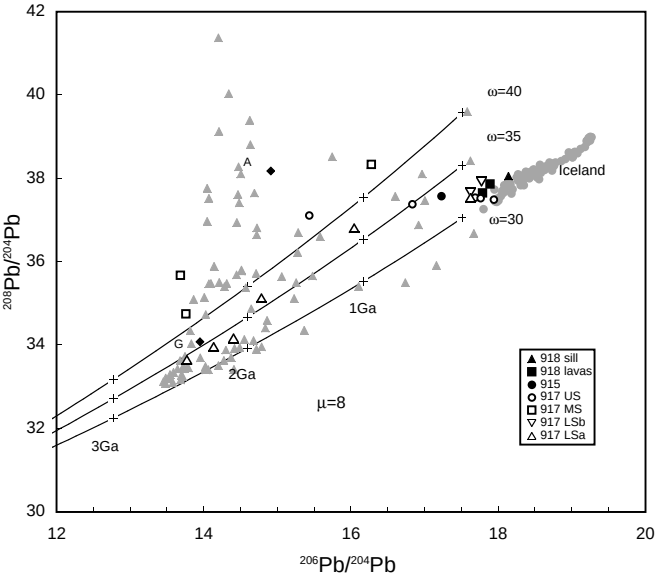

Figure 4. $^{208}Pb/^{204}Pb$ vs. $^{206}Pb/^{204}Pb$ in volcanic rock samples recovered from the Leg 152 transect (sample identification as in Fig. 1). The data have not been age corrected. The isotopic composition of Pb in volcanic rocks from Iceland (gray circles), Archaean basement rocks from East and southeast Greenland (gray triangles), and the average composition of granulite- (G) and amphibolite-facies (A) Lewisian gneiss are shown for comparison (data sources as in Fig. 3). Single-stage growth curves for $^{232}Th/^{204}Pb$ (ω) = 30, 35, and 40, all with $^{238}U/^{204}Pb$ (μ) = 8, are included for reference.

Series samples having more radiogenic $^{208}Pb/^{204}Pb$, relative to $^{206}Pb/^{204}Pb$, than the Lower Series samples.

DISCUSSION

Volcanic rocks erupted during breakup of the southeast Greenland margin show clear isotopic and elemental evidence for contamination of the magma, probably with continental crust. Contamination is most obvious in the pre-breakup volcanic rocks (Lower and Middle Series at Site 917) and falls off rapidly during the final stages of breakup (Fig. 2). This pattern of contamination resembles that described by Holm (1988) in the onshore Tertiary lavas of East Greenland, where the earliest lavas in the succession (the Vandfaldsdalen Formation) are the most contaminated. Holm (1988) used isotopic and elemental variation to argue that the magmas were contaminated with lithospheric mantle and that contamination from continental crust was of minor importance. The principal criteria used by Holm (1988) were apparent isotopic and chemical dissimilarities between the contaminants and local basement rocks, and the lack of a clear correlation between degree of differentiation and isotopic composition of the lavas. A lithospheric mantle source was inferred essentially by default.

The volcanic rocks analyzed in the present study show a much larger range of isotope ratios than do those analyzed by Holm (1988), and the effects of contamination are more clearly defined as a consequence. This probably reflects the more depleted character of the primitive magmas (Fitton et al., this volume), which made them more susceptible to the effects of contamination. It is clear from Figures 1, 3, and 4 that contamination with crustal rocks could explain the isotopic variation. Further evidence that continental crust was the principal contaminant comes from correlations between isotope ratios, indices of differentiation (e.g., SiO_2 content), and indices of contamination (e.g., incompatible trace-element ratios; Fitton et al., this volume). Figure 5 shows the correlation between $^{143}Nd/^{144}Nd$ and SiO_2 content for the Leg 152 volcanic rocks. The most evolved rocks are also the most contaminated, as would be expected from storage and differentiation of magma in crustal magma reservoirs.

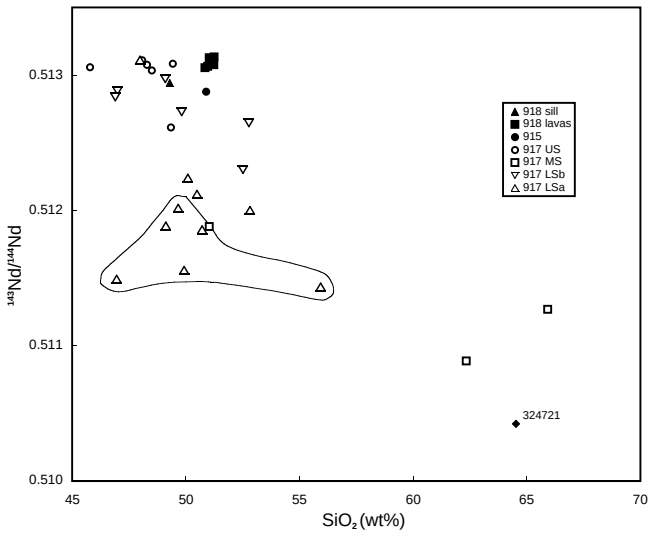

Figure 5. $^{143}Nd/^{144}Nd$ vs. SiO_2 (wt%) in volcanic rock samples recovered from the Leg 152 transect (sample identification as in Fig. 1). The field encloses data points representing samples from the lower part of the Lower Series at Site 917 (below Unit 73A), the oldest volcanic rocks recovered from the transect. SiO_2 data, recalculated on a volatile-free basis with all Fe as FeO, are from Fitton et al. (this volume).

At least two different contaminants must have been involved in the evolution of the southeast Greenland SDRS magmas. The first of these, which affected the six analyzed samples from the lower part of the Lower Series at Site 917 (below Unit 73A, Fig. 2), has low $^{87}Sr/^{86}Sr$, $^{143}Nd/^{144}Nd$, $^{206}Pb/^{204}Pb$, $^{207}Pb/^{204}Pb$, and $^{208}Pb/^{204}Pb$. These six samples define distinct fields on Figures 1 and 5, and show no correlation between $^{143}Nd/^{144}Nd$ and SiO_2 content (Fig. 5). The contaminant in these units *could* be lithospheric mantle, though its inferred isotopic and chemical characteristics are more consistent with lower crustal basic granulite. Evidence that continental crust, rather than lithospheric mantle, dominates the contaminant in these six samples is provided by their Pb-isotope ratios, with $^{206}Pb/^{204}Pb$ as low as 13.77 in sample 917-74A. Such extreme compositions have never been reported from mantle xenoliths, nor from lamproites or other basic igneous rocks thought to originate within the subcontinental lithospheric mantle. Lamproite, kimberlite, ultramafic lamprophyre, and carbonatite occurrences are widespread in West Greenland, and some of these rocks probably had a lithospheric mantle source (Larsen and Rex, 1992). Some mid-Proterozoic lamproites from West Greenland have extremely unradiogenic Pb, which may reflect the isotopic composition of their mantle source (Nelson, 1989), but even the *initial* $^{206}Pb/^{204}Pb$ of these rocks is not as low as that in sample 917-74A. Although it seems inevitable that the early SDRS magmas interacted with lithospheric mantle, the effects of this have almost certainly been swamped by the effects of crustal contamination.

Unit 73A in the Lower Series (Fig. 2) shows no evidence for contamination in its Sr-, Nd-, and Pb-isotope ratios (sample 917-73A, Table 2), and heralds a significant change in the nature of the contaminant. Units higher in the Lower Series represent magmas contaminated by crust with distinctly more-radiogenic Sr (Fig. 1). The change in the character of the contaminant above Unit 73A is also seen in the chemical composition of the lava flows of the Lower Series. Flows above Unit 73A have lower Sr/Zr, Ba/Zr, and La/Th than do flows lower in the succession (Fitton et al., this volume, fig. 10). A good negative correlation between $^{143}Nd/^{144}Nd$ and SiO_2 in these rocks (Fig. 5) provides strong evidence for contamination with silicic crust.

The transition from a low-$^{87}Sr/^{86}Sr$ to a high-$^{87}Sr/^{86}Sr$ contaminant occurred progressively from the lowest flows of the Lower Series through the Middle Series (Fig. 1). A large increase in $^{87}Sr/^{86}Sr$ with time is shown by the three analyzed Middle Series samples, collected from one of the lowest units (917-55), the central part (917-47), and the topmost unit (917-34B) of the series, respectively. Some of the olivine basalt and picrite flows of the Upper Series at Site 917, and the post-breakup lava flow sampled at Site 915, were also affected by a high-$^{87}Sr/^{86}Sr$, low-$^{143}Nd/^{144}Nd$ contaminant, but to a lesser extent (Fig. 1).

Evidence for a change in the nature of the contaminant with time also can be seen in the Pb-isotopic composition of the volcanic rocks. All of the contaminated rocks fall on a single array on a $^{207}Pb/^{204}Pb$ vs. $^{206}Pb/^{204}Pb$ diagram (Fig. 3), but show more scatter in $^{208}Pb/^{204}Pb$ (Fig. 4). Rocks from the upper part of the volcanic succession, notably the Middle Series at Site 917, show higher $^{208}Pb/^{204}Pb$, relative to $^{206}Pb/^{204}Pb$, than do those from the lower part (Fig. 4). This implies that the later magmas were contaminated with crust with higher time-integrated Th/U than were the earlier magmas, consistent with the observation (Fitton et al., this volume) of an abrupt decline in La/Th above Unit 74A in the Lower Series at Site 917.

The style of crustal contamination recorded in the southeast Greenland volcanic sequence closely resembles that which affected the contemporaneous magmas of the Hebridean igneous province of northwest Scotland, on the conjugate continental margin. Isotopic variation in these rocks can be modeled by variable contamination with granulite- and amphibolite-facies Lewisian gneiss (Carter et al., 1978; Dickin, 1981) representing, respectively, the lower and upper continental crust in this area. Dickin's (1981) average granulite- and amphibolite-facies Lewisian gneiss compositions provide plausible analogues for the contaminants in the southeast Greenland magmas (Figs. 1, 3, and 4). The Lewisian crust of northwest Scotland is very similar in its history and isotopic composition to that of southern Greenland (e.g., Kalsbeek et al., 1993). Published Pb-isotope ratios of Archaean basement rocks from East and southeast Greenland, plotted on Figures 3 and 4, are broadly comparable with data from the more contaminated volcanic rocks. Some of the volcanic rocks, however, have more extreme Pb-isotopic compositions than any of the crustal rocks, implying the presence of very unradiogenic Pb at depth in the crust.

The combined effects of crustal assimilation and fractional crystallization (AFC) can be modeled if the compositions of contaminant and uncontaminated primitive magma are known (DePaolo, 1981). The results of an attempt to do this for the southeast Greenland volcanic rocks are shown in Figure 6. The calculations were based on Zr and $^{143}Nd/^{144}Nd$ because both Zr and Nd are relatively immobile during alteration and both have partition coefficients close to zero for phases (principally olivine and plagioclase) likely to be involved in low pressure fractional crystallization. Furthermore, $^{143}Nd/^{144}Nd$ has approximately the same value in both granulite- and amphibolite-facies Lewisian rocks (Dickin, 1981), and in gneiss sample 324721 (Fig. 1). The primitive magma composition was estimated to have had 5 ppm Nd, 40 ppm Zr, and $^{143}Nd/^{144}Nd$ of 0.5131, based on the composition of the uncontaminated oceanic basalts from Site 918. Sample 324721 (Blichert-Toft et al., 1995; Fitton et al., this volume) was taken as the crustal contaminant.

It must be stressed that Figure 6 serves only to illustrate the possible effects of AFC processes and should not be taken too literally, because the chosen primitive magma and contaminant compositions will not be applicable to all samples. The sill at Site 918, for example, is less depleted in incompatible elements than are the other oceanic basalts, and its parental magma would have had higher concentrations of Zr and Nd. However, several observations can be made from this diagram. First, the lowest $^{143}Nd/^{144}Nd$ values seen in Lower Series lavas can be produced by simple bulk assimilation of 5%–10%

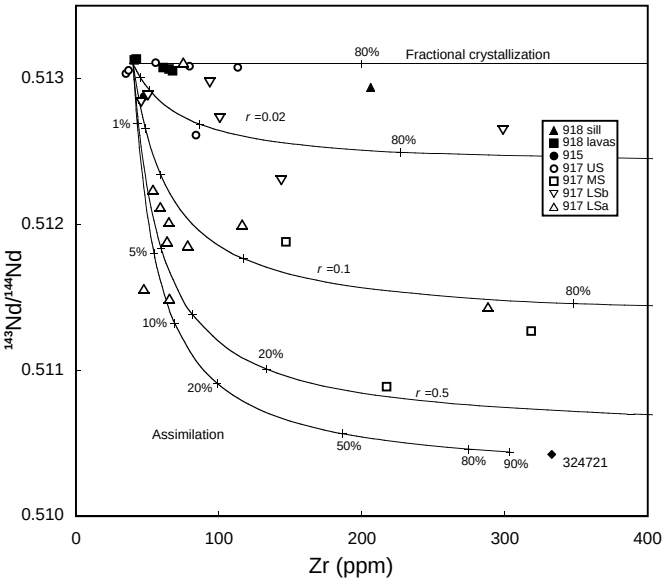

Figure 6. The effects on a primitive basaltic magma (40 ppm Zr, $^{143}Nd/^{144}Nd$ = 0.5131) of assimilation of crustal rocks (represented by sample 324721) coupled with fractional crystallization (after DePaolo, 1981). The top and bottom curves represent, respectively, the limiting cases of fractional crystallization without assimilation (with percentage crystallized), and bulk assimilation without fractional crystallization (with percentage crustal contaminant). The intermediate curves are for various ratios (*r*) of the rate of assimilation to the rate of fractional crystallization. The numbers on these curves indicate percentage crystallized. Sample identification as in Figure 1.

of the crustal component, without significant fractional crystallization. The bulk composition of sample 324721 is not strictly appropriate for the contaminant affecting the lower lavas of the Lower Series because its $^{87}Sr/^{86}Sr$ (0.7166; Blichert-Toft et al., 1995) is much too high (Fig. 1). The composition of a more appropriate partial melt from a more mafic lower crust would probably have lower concentrations of Zr and Nd than those in 324721. Lowering the Zr and Nd contents of the crustal component by a factor of two, to values similar to those in granulite-facies Lewisian leucogneiss (Weaver and Tarney, 1980), would double the amount of contaminant required. This level of contamination is comparable to the 15% deduced by Thompson et al. (1982) for the most contaminated basalts from Skye and Mull. Second, the Middle Series silicic rocks can be modeled by similar degrees of assimilation coupled with more extensive fractional crystallization. And third, the Upper Series olivine basalt and picrite magmas show evidence for some fractional crystallization with only minor assimilation of crust.

It is not possible to apply the same calculations to Pb-isotope ratios because the most contaminated basalts have slightly more-unradiogenic Pb than any of the analyzed crustal rocks (Figs. 3, 4). This implies either that the Pb in these volcanic rocks is entirely crustal in origin, or that crustal rocks containing even more-unradiogenic Pb exist at depth but have not been sampled at the surface in East or southeast Greenland. Highly unradiogenic Pb has been reported in the 3.7 Ga Amitsoq gneiss of southwest Greenland (Moorbath et al., 1975), and, similar material, if it exists in the southeast Greenland crust, could explain the unradiogenic Pb in lava flows from the lower part of the Lower Series. This would be a less satisfactory explanation, however, for the Middle Series volcanic rocks that have assimilated crust with high $^{87}Sr/^{86}Sr$ and therefore high time-integrated Rb/Sr. Such crust is unlikely to have very low U/Pb.

The problem of apparently large proportions of crustal Pb in relatively primitive basalt was also encountered by Dickin (1981) in his study of the Tertiary volcanic rocks of Skye. Dickin (1981) noted that some rocks showing no other evidence for contamination still contained a significant proportion of crustal Pb. He proposed that magmas can be selectively contaminated with Pb due to the greater mobility of this element. The close similarity in isotopic variation in the southeast Greenland and Hebridean Tertiary igneous suites has already been noted. Both show extreme levels of isotopic contamination with continental crust, to the extent that the original mantle isotopic signatures have been completely overprinted in many otherwise primitive basalts. This is probably because the uncontaminated primitive magmas in both provinces resembled N-MORB in their low incompatible-element concentrations (Wood, 1980; Thompson et al., 1982; Fitton et al., this volume) and both were therefore extremely susceptible to the effects of contamination. Magmatism in the Hebrides and southeast Greenland was initiated contemporaneously by lithospheric extension prior to continental breakup.

By analogy with Hebridean magmatism, the contaminant affecting the southeast Greenland magmas during continental extension and breakup seems to have changed, through time, from basic granulite-facies gneiss to amphibolite-facies gneiss. It is tempting, therefore, to conclude that the magma reservoirs moved to shallower depths in the crust over this period. A similar shallowing of magma reservoirs has been proposed for the East Greenland Tertiary lava successions, on the basis of basalt phase relations, by Fram and Lesher (1997). The nature of the crustal contaminant does not necessarily relate to depth of magma storage, because both granulite- and amphibolite-facies gneisses are exposed at the surface. However, the observed pattern of contamination could only be produced in magma stored at one level in the crust if amphibolite-facies gneiss were more refractory than granulite-facies gneiss. Even if this were so, it is unlikely that such a clear temporal pattern of contamination (Fig. 1) would result.

CONCLUSIONS

The magmas that gave rise to the SDRS off southeast Greenland were variably contaminated with continental crust. Volcanic rocks forming the pre-breakup succession closely resemble rocks from the Hebridean province in the nature and degree of contamination. Very low concentrations of incompatible elements made the uncontaminated primitive magmas in both provinces extremely sensitive to the effects of crustal contamination so that their original Sr-, Nd-, and Pb-isotopic ratios were easily overprinted by those of the crust. Contamination levels were generally high in the earliest SDRS magmas but declined rapidly during the final stages of continental breakup. Two distinct contaminants can be recognized in the isotopic and elemental composition of the volcanic rocks. One, with low $^{143}Nd/^{144}Nd$ and $^{87}Sr/^{86}Sr$, may be lower crustal basic granulite-facies gneiss, whereas the other, with low $^{143}Nd/^{144}Nd$ and high $^{87}Sr/^{86}Sr$, resembles upper crustal amphibolite-facies gneiss. Input from lithospheric mantle, as suggested by Holm (1988) for the onshore Tertiary volcanic rocks of East Greenland, cannot be excluded but is not required by the data. The contaminant changed with time through the pre-breakup volcanic succession; the earliest volcanic rocks were contaminated with granulite- and the later ones with amphibolite-facies gneiss. This suggests that magmas were stored at progressively shallower levels in the crust as lithospheric extension proceeded toward continental breakup.

ACKNOWLEDGMENTS

Financial support for this research was provided by the Natural Environment Research Council (grant GST/02/673). We are grateful to Anne Kelly and Vincent Gallagher, who provided expert technical assistance at SURRC, and to Charles Lesher and an anonymous reviewer for their constructive comments on the manuscript. Lotte Larsen, Mike Norry, and Andy Saunders are also thanked for helpful discussions on various aspects of the work.

REFERENCES

Barbero, L., Villaseca, C., Rogers, G., and Brown, P.E., 1995. Geochemical and isotopic disequilibrium in crustal melting: an insight from the anatectic granitoids from Toledo, Spain. *J. Geophys. Res.*, 100:15745–15765.

Blichert-Toft, J., Rosing, M.T., Lesher, C.E., and Chauvel, C., 1995. Geochemical constraints on the origin of the late Archean Skjoldungen alkaline igneous province, SE Greenland. *J. Petrol.*, 36:515–561.

Carter, S.R., Evensen, N.M., Hamilton, P.J., and O'Nions, R.K., 1978. Neodymium and strontium isotopic evidence for crustal contamination of continental volcanics. *Science*, 202:743–747.

Cohen, R.S., and O'Nions, R.K., 1982. The lead, neodymium and strontium isotopic structure of ocean ridge basalts. *J. Petrol.*, 23:299–324.

DePaolo, D.J., 1981. Trace element and isotopic effects of combined wallrock assimilation and fractional crystallization. *Earth Planet. Sci. Lett.*, 53:189–202.

Dickin, A.P., 1981. Isotope geochemistry of Tertiary igneous rocks from the Isle of Skye, N. W. Scotland. *J. Petrol.*, 22:155–189.

Elliott, T.R., Hawkesworth, C.J., and Grönvold, K., 1991. Dynamic melting of the Iceland plume. *Nature*, 351:201–206.

Fitton, J.G., Saunders, A.D., Larsen, L.M., Fram, M.S., Demant, A., Sinton, C., and Leg 152 Shipboard Scientific Party, 1995. Magma sources and plumbing systems during break-up of the Southeast Greenland margin: preliminary results from ODP Leg 152. *J. Geol. Soc. London*, 152:985–990.

Fram, M.S., and Lesher, C.E., 1997. Generation and polybaric differentiation of East Greenland Early Tertiary flood basalts. *J. Petrol.*, 38:231–275.

Furman, T., Frey, F.A., and Park, K.H., 1991. Chemical constraints on the petrogenesis of mildly alkaline lavas from Vestmannaeyjar, Iceland; the Eldfell (1973) and Surtsey (1963–1967) eruptions. *Contrib. Mineral. Petrol.*, 109:19–37.

Hards, V.L., Kempton, P.D., and Thompson, R.N., 1995. The heterogeneous Iceland plume: new insights from the alkaline basalts of the Snaefell volcanic centre. *J. Geol. Soc, London,* 152:1003–1009.

Hémond, C., Arndt, N.T., Lichtenstein, U., Hoffman, A.W., Oskarsson, N., and Steinthorsson, S., 1993. The heterogeneous Iceland plume: Nd:Sr:O isotopes and trace element constraints. *J. Geophys. Res.,* 98:15833–15850.

Holm, P.M., 1988. Nd, Sr and Pb isotope geochemistry of the Lower Lavas, East Greenland Tertiary Igneous Province. *In* Morton, A.C., and Parson, L.M. (Eds.), *Early Tertiary Volcanism and the Opening of the Northeast Atlantic*. Geol. Soc. Spec. Publ. London, 39:181–195.

Ito, E., White, W.M., and Göpel, C., 1987. The O, Sr, Nd and Pb isotope geochemistry of MORB. *Chem. Geol.,* 62:157–176.

Kalsbeek, F., Austrheim, H., Bridgwater, D., Hansen, B.T., Pedersen, S., and Taylor, P.N., 1993. Geochronology of Archaean and Proterozoic events in the Ammassalik area, South-East Greenland, and comparisons with the Lewisian of Scotland and the Nagssugtoqidian of West Greenland. *Precambrian Res.,* 62:239–270.

Larsen, H.C., Saunders, A.D., Clift, P.D., et al., 1994. *Proc. ODP, Init. Repts.*, 152: College Station, TX (Ocean Drilling Program).

Larsen, L.M., and Rex, D.C., 1992. A review of the 2500 Ma span of alkaline-ultramafic, potassic and carbonatitic magmatism in West Greenland. *Lithos*, 28:367–402.

Leeman, W.P., Dasch, E.J., and Kays, M.A., 1976. $^{207}Pb/^{206}Pb$ whole-rock age of gneisses from the Kangerdlugssuaq area, eastern Greenland. *Nature,* 263:469–471.

Moorbath, S., O'Nions, R.K., and Pankhurst, R.J., 1975. The evolution of early Precambrian crustal rocks at Isua, West Greenland: geochemical and isotopic evidence. *Earth Planet. Sci. Lett.,* 27:229–239.

Nelson, D.R., 1989. Isotopic characteristics and petrogenesis of the lamproites and kimberlites of central west Greenland. *Lithos,* 22:265–274.

Park, K.-H., 1990. Sr, Nd and Pb isotope studies of ocean island basalts: constraints on their origin and evolution [Ph.D. dissert.]. Columbia Univ., New York.

Sun, S.-S., and Jahn, B., 1975. Lead and strontium isotopes in post-glacial basalts from Iceland. *Nature,* 255:527–530.

Sun, S.-S., Tatsumoto, M., and Schilling, J.-G., 1975. Mantle plume mixing along the Reykjanes ridge axis: lead isotope evidence. *Science,* 190:143–147.

Taylor, P.N., Kalsbeek, F., and Bridgwater, D., 1992. Discrepancies between neodymium, lead and strontium model ages from the Precambrian of southern East Greenland: evidence for a Proterozoic granulite-facies event affecting Archaean gneisses. *Chem. Geol.,* 94:281–291.

Thompson, R.N., Dickin, A.P., Gibson, I.L., and Morrison, M.A., 1982. Elemental fingerprints of isotopic contamination of Hebridean Palaeocene mantle-derived magmas by Archaean sial. *Contrib. Mineral. Petrol.,* 79:159–168.

Weaver, B.L. and Tarney, J., 1980. Rare earth geochemistry of Lewisian granulite-facies gneisses, northwest Scotland: implications for the petrogenesis of the Archaean lower continental crust. *Earth Planet. Sci. Lett.,* 51:279–296.

Wood, D.A., 1980. The application of a Th-Hf-Ta diagram to problems of tectonomagmatic classification and to establishing the nature of crustal contamination of basaltic lavas of the British Tertiary volcanic province. *Earth Planet. Sci. Lett.,* 50:11–30.

Date of initial receipt: 24 May 1996
Date of acceptance: 16 August 1996
Ms 152SR-251